8

Analysis of an Endothermic Reaction in a Packed Column

8.1 Introduction

In 1977 the British Steel Corporation presented a problem to the European Study Groups for Industry, concerning the analysis of a gas–solid reaction in a column packed with solid catalyst pellets. This is an industrial problem of common concern, arising in various kinds of reactor such as a blast furnace. BSC were coy about the details of the reaction involved, but were happy to provide details of relevant physical parameters, essential for any analysis, and this allowed for a fairly thorough study of the problem.

Much of the applied mathematical interest in this type of problem has been motivated by the occurrence of *exothermic* reactions, i.e. those which release heat, as multiple steady states may exist for such reactions, and the associated phenomenon of thermal runaway can occur. However, the BSC problem concerned an *endothermic* reaction, one which absorbed heat, and our challenge thus lay in seeking some analytical understanding of the dynamics of the reaction.

The specific problem as summarised by BSC was as follows:

The problem is to solve two simultaneous partial differential equations. Although a method has been found using finite differences, the method is very slow in convergence and the boundary conditions have to be solved by an indirect manner. This is because the boundary conditions are dependent on an external radiative heat transfer problem. It would be very useful if an alternative approach to the problem was available in which the external heat transfer problem and the partial differential equations were formulated as a single problem.

Then, as now, the industry really wanted an efficient numerical code; and then, as now, our approach was directed towards analytical understanding. For a problem as simple as that stated below, it is in fact feasible to provide a good description of the solution analytically; furthermore, a numerical solution requires a certain amount of analytical pre-treatment, to know what time and

space steps should be used. In a sense, the challenge that this problem avoids raising, but which is also a suitable case for treatment, is the industrially relevant situation where ten, twenty, or a hundred reactions are going on. If we judge the state of the art by the extant literature (which is very substantial), then we find that much of the modelling and analysis that has been done is limited to the consideration of single-pellet dynamics, and also simple first- or second-order reaction kinetics (for examples of the gas–solid reaction literature, see [1], [3]–[6], [9]–[16], [18]–[22], [24], and [25]). It is thus perhaps a message yet to be realised, that applied analytic techniques can not only facilitate the solution of relatively simple problems such as that here, but are also capable of dealing with more realistic problems of practical concern.

8.2 The Problem and the Model

A cylindrical tube, of typical radius 10 cm and height 8 m, is packed with solid catalyst pellets, which react with a gas stream flowing through the tube. The situation is shown in figure 8.1.

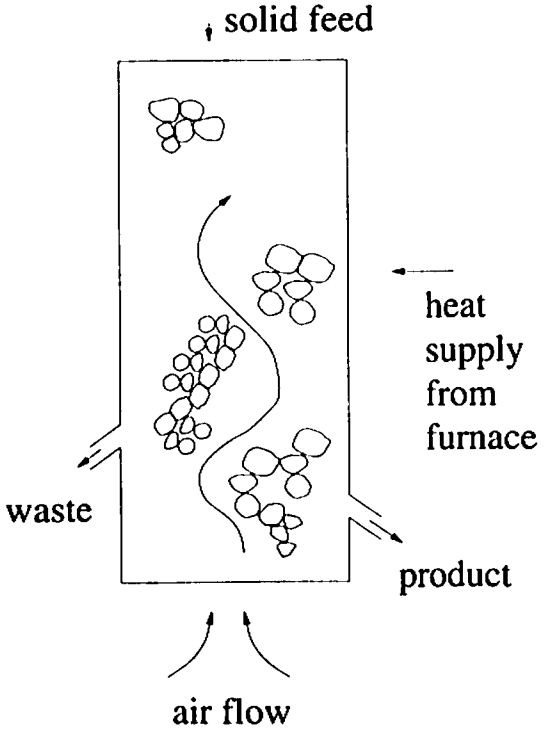

Fig. 8.1. A schematic illustration of the reactor geometry

A first-order reaction occurs between the gas and the solid, and the reaction is endothermic. If the solid pellets are sufficiently small, then the solid pellet temperature s may be taken to be locally uniform (within each pellet). It is always the case that the pellets are much smaller than the reactor radius, and it is commonly also the case that the pellets are in thermal equilibrium, and at relatively uniform temperature. In the present instance, this is confirmed *post hoc* by the fact that the macroscopic heat conduction parameter Γ is $O(1)$.

The gas (at mean temperature g) supplies heat to the solid through a viscous boundary layer (in the gas, next to the solid surface). For a typical gas velocity of 100 cm s^{-1}, pellet radius 1 cm, and gas viscosity 1 cm^2 s^{-1} (at reactor temperatures), the particle Reynolds number is 100, so that the flow would be laminar, although the irregular pore space is liable to make it highly unsteady. The Prandtl number of air at elevated temperatures is approximately one, so that the Peclet number is $\sim 10^2$, and a thermal boundary layer (slightly thicker than the viscous one) will exist next to the solid surface. It is not in fact essential that these boundary layers exist, since the model below will apply in any case, even if the particle Peclet number is small.

A steady-state model to describe this situation is

$$\begin{aligned} \rho_g c_p u \frac{\partial g}{\partial x} - h_v(s-g) &= k_g \nabla^2 g, \\ h_v(s-g) + \mathcal{R}\Delta H &= k_s \nabla^2 s, \\ u\frac{\partial c}{\partial x} &= -\mathcal{R}, \\ \mathcal{R} &= Kce^{-\lambda/s}, \end{aligned} \tag{8.1}$$

wherein u is the gas flux, ρ_g the gas density, and c_p the gas specific heat; h_v is a heat transfer coefficient (whose size will depend on the particle Reynolds and Peclet numbers), k_g and k_s are the effective thermal conductivities of gas and solid, and $\mathcal{R}$ is the reaction rate, given by $(8.1)_4$ for a first-order reaction; c is the gas reactant concentration, and ΔH is the heat of reaction absorbed per mole of reactant.

The first two equations represent heat transfer in the gas and solid phases. The terms in the gas temperature equation describe heat advection, interfacial heat transfer, and heat conduction respectively. In the second equation, the heat advection term is neglected on the basis that the solid velocity is negligible, so that heat conduction is balanced by the interfacial heat transfer and also the endothermic heat of reaction $\mathcal{R}\Delta H$. This term affects the solid temperature because the reaction occurs at the gas–solid interface. Depending on the nature of the pellet, this is either the pellet surface or, if the pellets

are porous, the internal surface area. In either event, the heat of reaction is removed from the solid.

The third equation represents the depletion of reactant in the gas stream. The rate of reaction $\mathcal{R}$ acts as a volume sink for the reactant, while the effect of diffusion can be ignored, being small. The final equation is the Arrhenius term for the rate of a first-order reaction, dependent on the solid (surface) temperature.

A good deal of physics is present in these equations, and we shall have some comments to make concerning the validity of the model in the discussion. For now we focus our attention on the model (8.1), supplemented by boundary conditions as indicated below. The inlet and outlet conditions are controlled by the rapid gas flow through the tube. In general, continuity of heat flux across a boundary has two components, due to advective flux and conductive heat transfer. When the advective term is large (as we suppose here), this essentially means that the temperature will be continuous. At the inlet, the gas flow carries in its external temperature, which we therefore consider prescribed, thus

$$g = s = g_0, \quad c = c_0 \quad \text{on} \quad x = 0, \tag{8.2}$$

where in addition we prescribe the entry reactant concentration of the gas stream. At the outlet, the same principle applies, except that the gas carries its temperature out of the tube. In the absence of any external control at the outlet, it is natural to suppose that there is no thermal boundary layer at the outlet, and a mathematically consistent way of ensuring this is to prescribe

$$\frac{\partial s}{\partial x} = \frac{\partial g}{\partial x} = 0 \text{ on } x = L, \tag{8.3}$$

although further consideration of the validity of this might be necessary in differing circumstances. In the present case, the outlet conditions will not actually affect the discussion.

Finally, on the wall,

$$\begin{aligned} k_g \frac{\partial g}{\partial r} &= h_0(T-g), \\ k_s \frac{\partial s}{\partial r} &= \varepsilon_G \sigma (T^4 - s^4). \end{aligned} \tag{8.4}$$

These Neumann boundary conditions differ in form because it is assumed that heat transfer to the gas from the wall at temperature T is by thermal conduction, whereas transfer to the solid pellets occurs through radiation; σ is the Stefan–Boltzmann constant and ε_G is the emissivity.

We nondimensionalise these equations by writing

$$g = g_0 + (T - g_0)g^*, \quad s = g_0 + (T - g_0)s^*,$$
$$x = r_0 x^*, \quad r = r_0 r^*, \quad c = c_0 c^*, \tag{8.5}$$

where r_0 is the tube radius. It is common in combustion theory to linearise the exponent in the Arrhenius exponential term (this is called the Frank–Kamenetskii approximation). The asymptotic basis on which this assumption ultimately rests is that the temperature variation in the problem is much less than the "activation" temperature λ (actually this is equal to the "activation energy" divided by the universal gas constant). In the example we use below, $\lambda = 5000$ K, whereas the external furnace temperature is 1300 K, and the inlet gas temperature is 700 K; thus the maximum temperature range is 600 K, much less than λ. The formal derivation requires

$$(T - g_0)s^* \ll g_0, \tag{8.6}$$

so that when the exponent is expanded to two terms of its Taylor series, we obtain

$$e^{-\lambda/s} \approx e^{-\lambda/g_0} e^{\Lambda s^*}, \tag{8.7}$$

where

$$\Lambda = \frac{\lambda(T - g_0)}{g_0^2}. \tag{8.8}$$

Apparently the assumption (8.6) is not supported by the values $T = 1300$ K and $g_0 = 700$ K, but in fact we later find that $s^* \sim 1/\Lambda$, so that (8.6) is equivalent to $g_0 \ll \lambda$, which *is* valid. The model (8.1) can then be written in the dimensionless form, dropping the asterisks,

$$\alpha \frac{\partial g}{\partial x} - (s - g) = \mu \nabla^2 g,$$
$$h(s - g) + c e^{\Lambda s} = \Gamma \nabla^2 s,$$
$$\frac{\partial c}{\partial x} = -\kappa c e^{\Lambda s}, \tag{8.9}$$

and the boundary conditions are

$$c = 1, \quad g = s = 0 \quad \text{on} \quad x = 0;$$
$$\frac{\partial g}{\partial x} = \frac{\partial s}{\partial x} = 0 \quad \text{on} \quad x = 1/\delta;$$

$$\gamma \frac{\partial g}{\partial r} = 1 - g,$$
$$\beta \frac{\partial s}{\partial r} = 1 - (\beta_1 + \beta_2 s)^4 \quad \text{on} \quad r = 1. \tag{8.10}$$

The parameters α, μ, h, Γ, κ, δ, γ, β, β_1, and β_2 are given by the values

$$\alpha = \frac{\rho_g c_p u}{h_v r_0}, \quad \mu = \frac{k_g}{h_v r_0^2},$$
$$h = \frac{h_v(T - g_0)}{\theta \Delta H}, \quad \Gamma = \frac{k_s(T - g_0)}{r_0^2 \theta \Delta H},$$
$$\kappa = \frac{\theta r_0}{u c_0}, \quad \delta = r_0/L,$$
$$\gamma = \frac{k_g}{h_0 r_0}, \quad \beta = \frac{k_s(T - g_0)}{r_0 \varepsilon_G \sigma T^4}, \quad \beta_1 = \frac{g_0}{T}, \quad \beta_2 = 1 - \beta_1, \tag{8.11}$$

where

$$\theta = K c_0 e^{-\lambda/g_0}. \tag{8.12}$$

Typical values of the parameters supplied by BSC were as follows:

$$\Delta H \sim 5.7 \times 10^4 \text{ cal mole}^{-1},$$
$$K \sim 0.9 \times 10^4 \text{ s}^{-1}, \quad \rho_g u \sim 1.9 \times 10^{-3} \text{ mole cm}^{-2} \text{ s}^{-1},$$
$$\lambda \sim 5 \times 10^3 \text{ K}, \quad c_0 \sim 0.4 \times 10^{-5} \text{ mole cm}^{-3},$$
$$u \sim 100 \text{ cm s}^{-1},$$
$$c_p \sim 0.2 \text{ cal mole}^{-1} \text{ K}^{-1}, \quad T \sim 1300 \text{ K}, \quad g_0 \sim 700 \text{ K},$$
$$r_0 \sim 10 \text{ cm}, \quad h_v \sim 2.3 \times 10^{-3} \text{ cal cm}^{-3} \text{ s}^{-1} \text{ K}^{-1},$$
$$k_g \sim 5 \times 10^{-4} \text{ cal cm}^{-1} \text{ s}^{-1} \text{ K}^{-1}, \quad k_s \sim 0.1 \text{ cal cm}^{-1} \text{ s}^{-1} \text{ K}^{-1},$$
$$h_0 \sim 5 \times 10^{-4} \text{ cal cm}^{-2} \text{ s}^{-1} \text{ K}^{-1}, \quad \varepsilon_G \sim 0.8,$$
$$\sigma \sim 1.37 \times 10^{-12} \text{ cal cm}^{-2} \text{ s}^{-1} \text{ K}^{-4}, \quad L \sim 800 \text{ cm}. \tag{8.13}$$

From these we find typical values of the constants to be

$$\alpha \sim 1.65 \times 10^{-2}, \quad \mu \sim 2.2 \times 10^{-3}, \quad \theta \sim 2.85 \times 10^{-5} \text{ mole cm}^{-3} \text{ s}^{-1},$$
$$h \sim 0.85, \quad \Gamma \sim 0.37, \quad \kappa \sim 0.72, \quad \delta \sim 1.25 \times 10^{-2},$$
$$\Lambda \sim 6, \quad \gamma \sim 0.1, \quad \beta \sim 1.9, \quad \beta_1 \sim 0.54, \quad \beta_2 \sim 0.46. \tag{8.14}$$

The presence of several small parameters suggests a variety of possible asymptotic limits, but before we proceed to their consideration, we append some comments on the model as supplied by the company.

Industrial Specification

The model as presented by BSC was not quite in the above form. The sign of the h_v term in $(8.1)_1$ was positive, the mass flow was given as $M = \rho_g u$, and the reaction equation for c was absent, with the heat absorption $\mathcal{R}\Delta H$ being given as $Q = Ae^{-\lambda/s}$. Presumably (it *was* over twenty years ago) the reaction equation for c was added during the study group, and a relevant value for ΔH was then applied. Presumably the gas is air and the gaseous reactant is oxygen (21% by volume). At 400°C, the density of air is about 0.5×10^{-3} gm cm^{-3}, and with its molecular weight being about 30 (gm mole^{-1}), this is a molar density of about 1.65×10^{-5} mole cm^{-3}, and 0.21 of this is 0.35×10^{-5} mole cm^{-3}, consistent with the supplied value. On the other hand, $M = \rho_g u$ must be the mass flow rate of air, so that the molar density ρ_g is about $5c_0$. If we use the supplied value of c_0, then we derive $u \sim 100$ cm s^{-1}. In fact, in the original report, a value of $u \sim 450$ cm s^{-1} was used, which reduces the value of κ by a factor 4.5. Presumably this oversight was due to neglect of what the gaseous reactant actually was.

Another comment worth making is that the heat transfer coefficient h_v and thermal conductivity k_s and k_g should be phase-averaged in some way (the superficial velocity u (i.e. the volume flux per unit area) is already effectively phase-averaged); no information is available as to whether this was in fact done, although it would only make cosmetic differences to the results.

The other parameters were supplied by BSC, though with some inaccuracies: r given as 1.38×10^{-2}, mass flow M as mole cm^{-2}.

8.3 Analysis

The original presentation of this problem was concerned, as is often the case, with the numerical solution of the model. The company had not nondimensionalised the model, and one can infer that the nature of their concern was such that the accurate solution of this *particular* model was perhaps less relevant than a qualitative understanding of how the model ought to be solved. In particular, the choice of a first-order reaction is presumably a gross simplification of the realistic chemistry. In this context, it ought to be pointed out that the inclusion of detailed chemistry is likely to lead to other, faster, reactions with associated short relaxation distances, and this will also cause difficulties in straightforward numerical schemes.

We now proceed to an analysis of the model. The parameter Λ is relatively large, particularly as it is present in an exponent. If we suppose that s is negative (and $O(1)$), then the heat absorption term is exponentially small and negligible. However, there is then no mechanism which can reduce s to such low values, and this assumption seems unwarranted. In a similar vein, if s is positive and $O(1)$, then the exponential term is dominant, suggesting to leading order either that $c \approx 0$ (which cannot be valid near the inlet), or that s is small and negative. And if this is the case, it seems likely that g also will be small and negative. This provides the motivation to rescale the temperatures to satisfy

$$g \sim s \sim \frac{1}{\Lambda}, \tag{8.15}$$

so that the corresponding dimensional temperature scales are g_0^2/λ. Of course we might have scaled this way initially, but it is more illuminating of the solution process to indicate the rescalings as they are discovered.

Adopting (8.15), the (rescaled) model is

$$\begin{aligned} \alpha g_x - (s - g) &= \mu \nabla^2 g, \\ H(s - g) + \frac{c}{\varepsilon} e^s &= \nabla^2 s, \\ c_x &= -\kappa c e^s, \end{aligned} \tag{8.16}$$

where

$$H = h/\Gamma \sim 2.2, \quad \varepsilon = \Gamma/\Lambda \sim 0.06, \tag{8.17}$$

with the side wall conditions being

$$\begin{aligned} \frac{\gamma}{\Lambda}\frac{\partial g}{\partial r} &= 1 - \frac{g}{\Lambda}, \\ \frac{\beta}{\Lambda}\frac{\partial s}{\partial r} &= 1 - \left(\beta_1 + \frac{\beta_2 s}{\Lambda}\right)^4 \quad \text{on} \quad r = 1, \end{aligned} \tag{8.18}$$

the other conditions being unaltered.

Outer Solution

The parameters α, μ, and ε are all small, and so we can neglect the corresponding terms in (8.16), an approximation that should be valid away from the boundaries:

$$s \approx g \approx \ln \varepsilon + S, \tag{8.19}$$

where S satisfies

$$\nabla^2 S = ce^S, \tag{8.20}$$

with boundary conditions to be determined below. The reactant concentration satisfies

$$c_x = -\varepsilon\kappa ce^S, \tag{8.21}$$

and suggests that the relevant length scale for the reaction is $x \sim 1/\varepsilon\kappa$. Apparently (but see below) this is comparable to the tube length $1/\delta$ (= 80; $1/\varepsilon \approx 16$, $\kappa < 1$), and we thus suppose that c varies slowly with x, so that it can be taken as independent of x in solving for S. In particular, away from the inlet, S is determined by solving

$$S_{rr} + \frac{1}{r}S_r = ce^S. \tag{8.22}$$

Wall Boundary Layers

For $\varepsilon \ll 1$, there is a boundary layer near $r = 1$ where S becomes large. We put

$$r = 1 - \sqrt{\varepsilon}R, \tag{8.23}$$

so that to leading order (back with s)

$$s_{RR} \approx ce^s, \tag{8.24}$$

with

$$-\frac{\partial s}{\partial R} \approx \nu \approx \frac{(1-\beta_1^4)\Lambda\sqrt{\varepsilon}}{\beta} \quad \text{on } R = 0. \tag{8.25}$$

Note that $\nu \approx 0.7$, so that $\nu = O(1)$. In order to match to the outer solution, we have to choose $s = s_0$ on $R = 0$, where

$$s_0 = \ln\frac{\nu^2}{2c}, \tag{8.26}$$

so that

$$s = -\ln\left(\frac{c}{2}\right) - 2\ln\left(R + \frac{2}{\nu}\right). \tag{8.27}$$

Writing this solution in terms of r and S implies that we require S in (8.22) to satisfy the matching condition

$$S \sim -\ln\frac{c}{2} - 2\ln(1-r) \quad \text{as } r \to 1. \tag{8.28}$$

Suppose, for simplicity, that in fact $c \approx c(x)$. Then

$$S \approx \ln\frac{8}{c} - 2\ln(1-r^2). \tag{8.29}$$

Thus, in the variables scaled by g_0^2/λ (≈ 70 K), the centre line (minimum) temperature is

$$s \approx \ln[8\varepsilon/c], \tag{8.30}$$

while the solid temperature at the wall is

$$s_0 \approx \ln\left[\frac{\varepsilon\Lambda^2(1-\beta_1^4)^2}{2c\beta^2}\right]. \tag{8.31}$$

Gas Temperature Boundary Layer

Evidently, the assumption $\varepsilon \ll 1$ is hardly relevant to the above solution, since S can be found (for $c = c(x)$) explicitly. For the gas thermal boundary layer we put

$$r = 1 - \sqrt{\mu}\eta, \tag{8.32}$$

and if $\sqrt{\mu} \ll \sqrt{\varepsilon}$, then $s \approx s_0$ and to satisfy the approximate condition

$$-\frac{\gamma}{\Lambda\sqrt{\mu}}g_\eta \approx 1, \tag{8.33}$$

we have

$$g \approx s_0 + \frac{\Lambda\sqrt{\mu}}{\gamma}e^{-\eta}, \tag{8.34}$$

while the gas temperature at the wall is

$$g_0 \approx s_0 + \frac{\Lambda\sqrt{\mu}}{\gamma}. \tag{8.35}$$

Inlet Boundary Layers

We omit details. There will be an adjustment layer for s of thickness $O(\sqrt{\varepsilon})$ and a thinner layer for g of thickness $\sqrt{\mu}$ (since $\sqrt{\mu} \gg \alpha$). In addition, (8.29) becomes valid (if $c = c(x)$) for distances $x \gg 1$, i.e. beyond the inlet region.

Temperature and Reactant Profiles

From (8.27) and (8.28), we can write a uniform approximation to the particle temperature as

$$s \approx \ln \frac{8\varepsilon}{c} - 2\ln\left[1 - r^2 + \frac{2\sqrt{\varepsilon}}{\nu}\right], \tag{8.36}$$

and the reactant concentration then satisfies (8.21), with s given as above. From this we have

$$c \approx 1 - \frac{8\varepsilon\kappa x}{\left(1 - r^2 + \frac{2\sqrt{\varepsilon}}{\nu}\right)^2}, \tag{8.37}$$

and the reaction zone boundary (where $c = 0$) is given by

$$x \approx \frac{\left(1 - r^2 + \frac{2\sqrt{\varepsilon}}{\nu}\right)^2}{8\varepsilon\kappa}, \tag{8.38}$$

and is shown in figure 8.2. The maximum extent of the reaction zone at the centre line is

$$x_m \approx \frac{\left(1 + \frac{2\sqrt{\varepsilon}}{\nu}\right)^2}{8\varepsilon\kappa}. \tag{8.39}$$

Similarly, a uniform expansion for the dimensionless gas temperature is

$$g \approx s + \frac{\Lambda\sqrt{\mu}}{\gamma} \exp\left[-\frac{(1-r)}{\sqrt{\mu}}\right]. \tag{8.40}$$

Figure 8.3 shows the cross-sectional profiles of the solid temperature given by (8.36) and (8.37) at various values of x. The core temperature varies slowly with x, while the solid warms up at the wall as the reaction proceeds. After the reaction front leaves the wall at $x \approx 1.4$, the core temperature begins to increase as the reactive core shrinks towards the centre. Figure 8.4 compares gas and solid temperatures given by (8.36), (8.37) and (8.40) at $x = 0.2$ near the tube inlet. The temperatures are the same in the core, but the gas has a hot boundary layer at the tube wall due to its relatively low thermal conductivity (as indicated by the low value of μ).

It is apparent that the solution for s becomes invalid if $c \to 0$ at the wall, since s must be bounded (by Λ) there, in contrast to (8.31), which indicates $s_0 \to \infty$ as $c \to 0$. At the wall, (8.37) implies that $c = c_0$ satisfies

$$c_0 \approx 1 - 2\nu^2\kappa x, \tag{8.41}$$

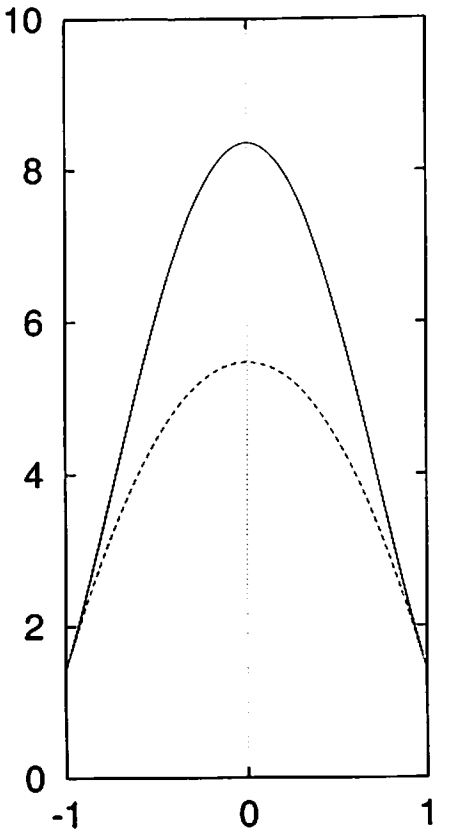

Fig. 8.2. The reaction zone given by the crude approximation (8.38) (solid curve), as well as the more accurate expression (8.52) (broken curve), with $\varepsilon = 0.06$, $\kappa = 0.72$, and $\nu = 0.7$

with a termination front at $x_0 = 1/2\nu^2\kappa$. Beyond the reaction front, we can expect a dead zone where $c = 0$, and in fact we see that the approximation for s is invalid for $x \gg 1$, both because (8.37) implies c depends on r, and also because of the dead zone. Despite this, we might expect the general characteristics of the reaction zone to be similar to that described here; that is to say, a central reactive core of inverted paraboloidal shape (as in figure 8.2) in which the gas and solid temperatures are depressed.

Reaction Front

The preceding analysis with $c = c(x)$ is inaccurate at large x but suggestive of the existence of a well-defined front at $r = r_f(x)$, say. If we now suppose

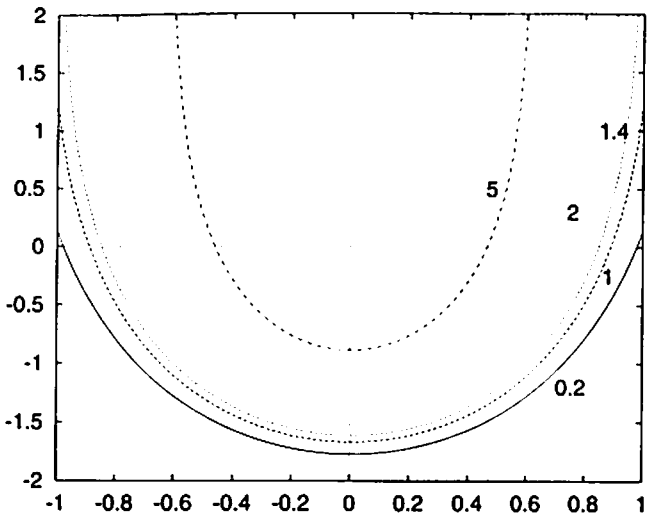

Fig. 8.3. Profiles of s versus r given by (8.36) and (8.37) for values of x chosen as 0.2, 1, 1.4, 2, 5, and with $\varepsilon = 0.06$, $\kappa = 0.72$, and $\nu = 0.7$. The reaction terminates on the wall at $x_0 \approx 1.417$, so that the profiles for $x = 2$ and $x = 5$ are not strictly accurate, though they do represent the qualitative behaviour of the solution

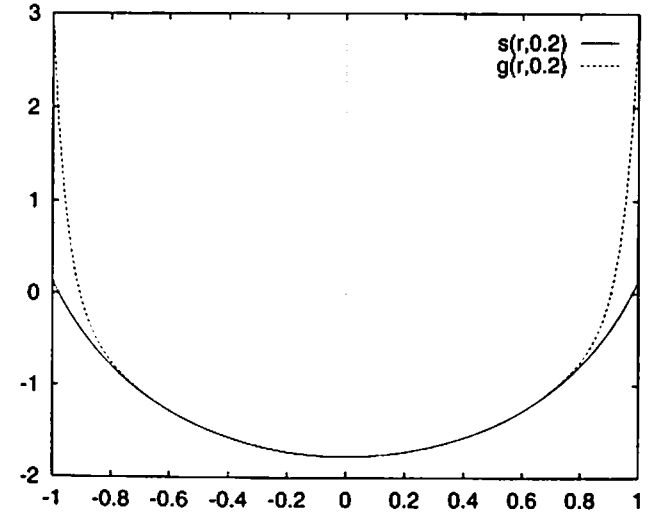

Fig. 8.4. A comparison of the gas and solid temperatures across the tube, at $x = 0.2$. The parameter values used are $\varepsilon = 0.06$, $\kappa = 0.72$, $\nu = 0.7$, $\Lambda = 6$, $\mu = 2.2 \times 10^{-3}$, and $\gamma = 0.1$

$c = c(x, r)$, then the problem we have to solve in $r < r_f$ for s and c is

$$\frac{c}{\varepsilon} e^s = s_{rr} + \frac{1}{r} s_r + s_{xx},$$

$$c_x = -\kappa c e^s, \tag{8.42}$$

with $c = 1$ on $x = 0$, and

$$\frac{\partial s}{\partial r} \approx \frac{\nu}{\sqrt{\varepsilon}} \quad \text{on } r = 1. \tag{8.43}$$

The solution with $c = c(x)$ is in fact valid so long as $\varepsilon\kappa x \ll 1$, and in particular while c_0 (on the wall, see (8.41)) is greater than zero, i.e. $x < x_0 = 1/2\nu^2\kappa$. For $x > x_0$, we suppose that $c = 0$ in $r > r_f$, so that

$$s = s_0 + \frac{\nu}{\sqrt{\varepsilon}} \ln r, \quad r > r_f, \tag{8.44}$$

and the problem to determine r_f and s_0 is found from the solution for S $(= s - \ln \varepsilon)$ of

$$ce^S = S_{rr} + \frac{1}{r} S_r,$$

$$c_x = -\varepsilon\kappa c e^S, \tag{8.45}$$

with

$$c = 1 \quad \text{on} \quad x = 0, \quad c = 0 \quad \text{and} \quad S_r = \frac{\nu}{\sqrt{\varepsilon} r_f} \quad \text{on} \quad r = r_f. \tag{8.46}$$

It is straightforward to solve this problem numerically. Although

$$\nu/\sqrt{\varepsilon} \approx 3$$

is hardly large, it is useful to take the limit $\sqrt{\varepsilon} \ll 1$ seriously. In this case, a genuine reaction front exists. We revert to the variable s, and put

$$r = r_f - \sqrt{\varepsilon} R \tag{8.47}$$

(cf. (8.23)), so that, to leading order,

$$s_{RR} \approx ce^s,$$

$$\rho c_R \approx ce^s, \tag{8.48}$$

where we define

$$r_f' = -\kappa\sqrt{\varepsilon}\rho \ll 1. \tag{8.49}$$

Thus the reaction zone will be of length $O(1/\kappa\sqrt{\varepsilon})$ in this case, and we can take $c \approx 1$ in $r < r_f$, so that suitable boundary conditions for matching purposes are

$$s \sim s^* - \frac{\nu}{r_f} R, \quad c \to 0 \quad \text{as} \quad R \to -\infty;$$
$$s_R \to 0, \quad c \to 1 \quad \text{as} \quad R \to +\infty : \tag{8.50}$$

here (cf. (8.44))

$$s^* = s_0 + \frac{\nu}{\sqrt{\varepsilon}} \ln r_f. \tag{8.51}$$

It follows that $\rho = \nu/r_f$, and thus from (8.49),

$$r_f^2 = 1 - 2\kappa\sqrt{\varepsilon}\nu(x - x_0), \tag{8.52}$$

where x_0 is given by $x_0 = 1/2\nu^2\kappa$ (see (8.41)), and also

$$c = 1 + \frac{s_R}{\rho}. \tag{8.53}$$

Thus s satisfies

$$s_{RR} \approx \left(1 + \frac{s_R}{\rho}\right) e^s, \tag{8.54}$$

with first integral

$$s_R - \rho \ln\left(1 + \frac{s_R}{\rho}\right) = \frac{1}{\rho} e^s; \tag{8.55}$$

the constant of integration has been chosen uniquely so that a monotone decreasing trajectory exists with $s_R \to 0$ as $R \to \infty$. The solution of (8.54) can be written parametrically as

$$s = 2\ln\rho + \ln[\xi - 1 + e^{-\xi}],$$
$$R = \frac{1}{\rho}\int_\xi^K \frac{du}{u - 1 + e^{-u}}, \tag{8.56}$$

where $\xi > 0$, and the value of K simply fixes the origin. For example, if we choose $c = \frac{1}{2}$ at $R = 0$, then $K = \ln 2$. The value of s_0 is then fixed via (8.50), together with the behaviour of (8.55) as $R \to -\infty$ ($\xi \to \infty$); we find

$$s_0 = \frac{\nu}{\sqrt{\varepsilon}} \ln\frac{1}{r_f} + \ln K + 2\ln\frac{\nu}{r_f} - \int_K^\infty \frac{(1 - e^{-u})du}{u(u - 1 + e^{-u})}, \tag{8.57}$$

so the wall temperature increases as the reacting core shrinks.

In $r < r_f$, $S = s - \ln\varepsilon$ then satisfies (with $c \approx 1$)

$$S_{rr} + \frac{1}{r} S_r = e^S \tag{8.58}$$

as before, with the matching condition obtained from (8.54),

$$S \sim \ln 2 - 2\ln(r_f - r) \quad \text{as} \quad r \to r_f, \tag{8.59}$$

with solution

$$S = \ln\left[\frac{8r_f^2}{(r_f^2 - r^2)^2}\right]. \tag{8.60}$$

8.4 Discussion

This basically concludes the analysis. We now have a good idea of how the solution behaves. There is a detailed reactive core of dimensional length (from (8.51)) $\approx (2\kappa\nu\sqrt{\varepsilon})^{-1} r_0$. Ignoring $\beta_1^4 \ll 1$, this is

$$x_c \approx \frac{\beta r_0}{2\kappa\Gamma} = \frac{u c_0 r_0 \Delta H}{2\varepsilon_G \sigma T^4}. \tag{8.61}$$

There is a preceding attached reactive core of length $x_a \approx (2\nu^2\kappa)^{-1} r_0$; this is

$$x_a \approx \frac{\beta^2}{2\kappa\Lambda\Gamma} = \frac{u c_0 g_0^2 k_s \Delta H}{2\lambda\varepsilon_G^2\sigma^2 T^8}. \tag{8.62}$$

In the reactive core, the temperature is low, and if the radiative heat flux is high enough ($\nu/\sqrt{\varepsilon} \gg 1$, i.e. $\Lambda \gg \beta$, i.e.

$$\frac{\lambda r_0 \varepsilon_G \sigma T^4}{g_0^2 k_s} \gg 1), \tag{8.63}$$

then the reaction occurs in a thin front.

There are three concluding statements to make concerning the success of this case study. Firstly, it is a good illustration of the efficacy of applied mathematics. In a matter of days, an experienced researcher can essentially solve this problem far beyond the ability of a numerical solution. Numerical solution of this problem is best provided as an illustration and confirmation of the analytic results.

Secondly, did this study answer the question *as posed* in the introduction? The answer is yes, in passing. One only has to nondimensionalise the equations to realise that the existence of thermal boundary layers at the walls

and inlet will cause particular problems in devising numerical methods. This problem is best analysed first, and solved numerically later.

But the third and most significant observation is that all the analytic effort devoted to solving this problem in 1977 was directed towards solving the wrong problem. The model provided by BSC included the heat of reaction term $\mathcal{R}\Delta H$ in the *gas* temperature equation ($(8.1)_1$, not $(8.1)_2$). In addition the Arrhenius term was written in terms of the *gas* temperature, not the solid temperature. The consequent nature of the solution was quite different in its detail; for example $s = g$ was no longer appropriate.

Aris's two volumes [2] had appeared, as had Szekely et al.'s book [23]. They gave a comprehensive description of just this kind of problem. But the assembled applied analysts failed, in fact, to devote sufficient attention to the correct modelling of the problem, in their zeal to get on with its solution. If there is a lesson to be learned here, it is that one should never seek to solve fancy problems without a decent understanding of the appropriate physical processes.

8.5 Further Modelling Considerations

The reaction between a gas stream and a solid catalyst pellet is a surface reaction; it may occur at the pellet surface, or within the pellet if it is permeable. The simplest case is the "shrinking unreacted core" model, where the pellet is impermeable, and the heat of reaction is absorbed at the surface; see [23] or [8] for a discussion of this. It is then appropriate to include the heat absorption in the s equation, as we have done here, together with the macroscopic heat conduction term, since we can assume (since $\Gamma \sim 1$) that the pellets are in local thermal equilibrium.

The choice of the reaction rate $\mathcal{R}$ in (8.1) also omits any consideration of the surface nature of the reaction. In fact the conservation of gas reactant in $(8.1)_3$ would prescribe the supply from the gas stream to the particles, thus

$$u\frac{\partial c}{\partial x} = -h_c(c - c_s), \tag{8.64}$$

where h_c is a mass transfer coefficient, and c_s the pellet surface gas concentration. A first-order reaction would then prescribe the reaction rate as

$$\mathcal{R} = Kc_s e^{-\lambda/s}, \tag{8.65}$$

and it remains to determine c_s. (More generally c_s would be replaced by the fraction of adsorbed sites at the surface, but at low values of c_s, this is proportional to c_s, at least for the Langmuir isotherm.)

Finally, the rate of supply must equal the rate of reaction, so that

$$c_s = \frac{c}{1 + (K/h_c)e^{-\lambda/s}}. \tag{8.66}$$

In particular, we regain (8.1) if h_c is large enough; otherwise, the Arrhenius factor is modified.

Further understanding of how the surface reaction term is included requires a discussion of the detailed pellet dynamics. This is discussed in [23], and is lucidly reviewed in [17] and [7]. For the simplest model, the nonporous pellet alluded to above, the reaction causes the pellets to shrink. For complete gasification, or if any resulting ash is removed by spalling, the pellet size is given by the dimensionless radius ξ (= 1 initially), and this varies as the reaction proceeds. The volumetric rate of reaction then depends on ξ (see [8], pp. 195 ff.), and in a steady-state model the time evolution of ξ is described by an advective evolution equation which incorporates the solid's settling velocity.

The other type of pellet model describes porous pellets. When the pellet is formed from compacted grains, this is also referred to as a grain model. Following [8], the dimensionless temperature and concentration fields in a porous (compacted grain) pellet can be written in the form

$$\begin{aligned} \theta_t &= \nabla^2\theta - \beta r, \\ c_t &= \frac{1}{Le}\nabla^2 c - \mu r, \end{aligned} \tag{8.67}$$

where the length scale is the pellet radius. If we realistically assume $\mu \ll 1$, then the pellet temperature θ is quasi-steady; and if also $\beta \ll 1$, then the pellets are isothermal. In this case, the evolution of the reaction in the pellet can be described through the reactant equations

$$\begin{aligned} \delta\frac{\partial c}{\partial \tau} &= \frac{1}{\phi^2}\nabla^2 c - c\xi^{F_g - 1}H(\xi), \\ \frac{\partial \xi}{\partial \tau} &= -cH(\xi) \end{aligned} \tag{8.68}$$

for a first-order reaction. The pellet temperature is normalised to zero here. In these equations, ξ is the (dimensionless) grain (not pellet) radius, $H(\xi)$ is the Heaviside step function, $\delta = c_s/\rho_s$ is the ratio of gas molar concentration to solid molar concentration, $\tau = \delta\mu t$, and $\phi = \{\mu Le\}^{1/2}$ is the Thiele modulus.

The exponent F_g represents grain shape, being equal to 1, 2, or 3 for plates, cylinders, or spheres respectively.

Realistically, $\delta \ll 1$, and the time derivative of c can be ignored (the quasi-static assumption). In general, solutions must be numerical, but analytic results are possible for large or small Thiele modulus. If $\phi \ll 1$ (chemical control), the reactant concentration is uniform in the pellet, and reaction proceeds uniformly throughout. More interesting mathematically is the diffusion-controlled limit $\phi \gg 1$, when a reaction front moves into the pellet (see below).

Many other aspects of the modelling may be considered as exercises. For example:

- Why does the fact that $\Gamma \sim 1$ imply that we can assume that pellets are in thermal quasi-equilibrium?
- Follow the discussion in [8] to modify the model (8.1) to allow for shrinking nonporous pellets, and examine the effect of this modification on the analysis presented here.
- Use the discussion in [8] (pp. 190 ff.) and [23] (pp. 133 ff.) to derive (8.68). For the quasi-static chemically controlled pellet, derive the appropriate form of the heat sink term in (8.1).
- Show that for the quasi-static diffusionally controlled pellet with spherical grains ($F_g = 3$), a reaction front at $r = r_f$, which separates a reacted fringe ($\xi = 0$) from an unreacted core ($c \approx 0$, $\xi \approx 1$), moves into the pellet at a rate

$$\dot{r}_f \approx -\frac{3}{\phi^2 r_f (1 - r_f)}.$$

Deduce the corresponding form of the heat sink term in (8.1).

References

[1] Adrover, A. & Giona, M. (1997) Solution of unsteady-state shrinking-core models by means of spectral/fixed-point methods: nonuniform reactant distribution and nonlinear kinetics. Ind. Eng. Chem. Res. **36**, 2452–2465.

[2] Aris, R. (1975) *Mathematical Theory of Diffusion and Reaction in Permeable Catalysts*, (2 volumes), Oxford University Press.

[3] Bhatia, S. K. (1985) On the pseudo-steady state hypothesis for fluid solid reactions. Chem. Eng. Sci. **40**, 868–872.

[4] Bhatia, S. K. (1991) Perturbation analysis of gas-solid reactions. 2. Reduction to the diffusion-controlled shrinking core. Chem. Eng. Sci. **46**, 1465–1474.

[5] Cao, G., Varma, A. & Strieder, W. (1993) Approximate solutions for nonlinear gas-solid noncatalytic reactions. AIChE J. **39**, 913–917.

[6] Chan, Y. H. & McElwain, D. L. S. (1996) Asymptotic analysis and effect of reaction order on a reversible gas-solid system with fast reaction. J. Eng. Math. **30**, 365–386.

[7] Doraiswamy, L. K. & Sharma, M. M. (1984) *Heterogeneous Reactions: Analysis, Examples and Reactor design, Vol. 1*. John Wiley, New York, USA.

[8] Fowler, A. C. (1997) *Mathematical Models in the Applied Sciences*, Cambridge University Press, England.

[9] Hahn, Y. B. & Chang, K. S. (1998) Mathematical modelling of the reduction process of iron ore particles in two stages of twin-fluidized beds connected in series. Metall. Mater. Trans. B **29**, 1107–1115.

[10] Jamshidi, E. & Ebrahim, H. A. (1996) An incremental analytical solution for gas-solid reactions, application to the grain model. Chem. Eng. Sci. **51**, 4253–4257.

[11] Lédé, J. & Villermaux, J. (1993) Comportement thermique et chimique de particules solides subissant une réaction de décomposition endothermique sous l'action d'un flux de chaleur externe. Can. J. Chem. Eng. **71**, 209–217.

[12] Liu, F., McElwain, D. L. S. & Donskoi, E. (1998) The use of a modified Petrov-Galerkin method for gas-solid reaction modelling. IMA J. Appl. Math. **61**, 33–46.

[13] Lu, H. B., Mazet, N., Coudevylle, O. & Mauran, S. (1997) Comparison of a general model with a simplified approach for the transformation of solid-gas media used in chemical heat transformers. Chem. Eng. Sci. **52**, 311–327.

[14] Lu, H. B., Mazet, N. & Spinner, B. (1996) Modeling of gas-solid reaction—coupling of heat and mass transfer with chemical reaction. Chem. Eng. Sci. **51**, 3829–3845.

[15] Patisson, F., Francois, M. G. & Ablitzer, D. (1998) A non-isothermal, non-equimolar transient kinetic model for gas-solid reactions. Chem. Eng. Sci. **53**, 697–708.

[16] Pritsker, M. D. (1996) Shrinking core model for systems with facile heterogeneous and homogeneous reactions. Chem. Eng. Sci. **51**, 3631–3645.

[17] Ramachandran, P. A. & Doraiswamy, L. K. (1982) Modeling of non-catalytic gas-solid reactions. AIChE J. **28**, 881–900.

[18] Rode, H., Orlicki, D. & Hlavacek, V. (1995) Reaction-rate modelling in noncatalytic gas-solid systems—species transport and mechanical stress. AIChE J. **41**, 2614–2624.

[19] Shah, N. & Ottino, J. M. (1987) Transport and reaction in evolving, disordered composites. 1. Gasification of porous solids. Chem. Eng. Sci. **42**, 63–72.

[20] Shankar, K. & Yortsos, Y. C. (1983) Asymptotic analysis of single pore gas-solid reactions. Chem. Eng. Sci. **38**, 1159–1165.

[21] Sohn, H. Y. & Chaubal, P.C. (1986) Approximate closed-form solutions to various model equations for fluid-solid reactions. AIChE J. **32**, 1574–1578.

[22] Sohn, H. Y., Johnson, S. H. & Hindmarsh, A. C. (1985) Application of the method of lines to the analysis of single fluid-solid reactions in porous solids. Chem. Eng. Sci. **40**, 2185–2190.

[23] Szekely, J., Evans, J. W. & Sohn, H. Y. (1976) *Gas-Solid Reactions*, Academic Press, New York, USA.

[24] Taylor, P. R., Dematos, M. & Martins, G. P. (1983) Modeling of non-catalytic fluid-solid reactions—the quasi-steady state assumption. Metall. Trans. B **14**, 49–53.

[25] Zhou, L. & Sohn, H. Y. (1996) Mathematical modelling of fluidized-bed chlorination of rutile. AIChE J. **42**, 3102–3112.

Andrew C. Fowler
OCIAM
Mathematical Institute, 24–29, St. Giles, Oxford OX1 3LB, UK
fowler@maths.ox.ac.uk